J Fluoresc (2015) 25:103–112
DOI 10.1007/s10895-014-1485-x

ORIGINAL PAPER

Structural and Photophysical Properties of (2E) -3-[4-(Dimethylamino) Phenyl]-1-(Naphthalen-1-yl) Prop-2-en-1-One (DPNP) in Different Media

Mehboobali Pannipara · Abdullah M. Asiri · Khalid A. Alamry · Ibrahim A. Salem · Samy A. El-Daly

Received: 21 September 2014 / Accepted: 1 December 2014 / Published online: 25 January 2015

Abstract The spectral and photophysical properties of a new chalcone derivative (2E)-3-[4-(dimethylamino) phenyl]-1-(naphthalen-1-yl) prop-2-en-1-one (DPNP) containing donor-acceptor group has been synthesized and characterized on the basis of the spectral (IR, ^{1}HNMR & ^{13}C NMR) and X-ray crystallographic data. The effect of solvents on photophysical parameters such as singlet absorption, molar absorptivity, oscillator strength, dipole moment, fluorescence spectra, and fluorescence quantum yield of DPNP have been investigated comprehensively. Significant red shift was observed in the emission spectrum of DPNP compared to the absorption spectrum upon increasing the solvent polarity, indicating a higher dipole moment in the excited state than in the ground state. The difference between the excited and ground state dipole moments ($\Delta\mu$) were obtained from Lippert-Mataga and Reichardts correlations by means of solvatochromic shift method. The effects of medium acidity on the electronic absorption and emission spectra of DPNP were studied. The interaction of DPNP with colloidal silver nanoparticles (AgNPs) was also studied in ethanol and ethylene glycol using steady state fluorescence quenching measurements. The fluorescence quenching data reveal that dynamic quenching and energy transfer play a major role in the fluorescence quenching of DPNP by Ag NPs.

M. Pannipara · A. M. Asiri · K. A. Alamry · S. A. El-Daly (✉)
Department of Chemistry, Faculty of Science, King Abdulaziz University, P.O. Box 80203, Jeddah 21589, Saudi Arabia
e-mail: samyeldaly@yahoo.com

A. M. Asiri
Center of Excellence for Advanced Materials Research, King Abdulaziz University, Jeddah 21589, P.O. Box 80203, Saudi Arabia

I. A. Salem · S. A. El-Daly
Department of Chemistry, Faculty of Science, Tanta University, 31527 Tanta, Egypt

Keywords Chalcone · Effect of solvents · Physicochemical parameters · Fluorescence quenching · Effect of acidity

Introduction

The photophysical properties of fluorophores containing donor and acceptor groups separated by an ethenyl or keto-vinyl bridge have attracted considerable research attention owing to their promising applications in diverse fields due to intramolecular charge transfer (ICT) [1]. The ICT state depends mainly on the substituent effect, solvent polarity and temperature, hence their photophysical properties can be exploited in many potential applications such as sensing, organic light-emitting diodes, laser and fluorescent dyes [2–5]. Apart from the biological and pharmacological aspects, the spectral and photophysical properties of chalcones, a class of compound with strong electron donor-acceptor interactions in which donor and acceptor moieties are separated by a keto-vinyl bridge, are of continuing research interest due to their different degrees of charge transfer that are sensitive to the micro environment.

It is well-known that physical properties of solvents such as polarity, polarizability and dielectric constant will affect a chemical process in which they are carried out. The absorption and emission bands of fluorescent organic molecules which carry a charge centre depend on the polarity of the solvent and hence their interaction with different media offers an insight to their excited state [6–10]. Although there are many methods to determine the ground and excited state dipole moments of a molecule, solvent shift method based on absorption and emission intensity is the most accepted one [11].

Interaction of metallic nanoparticles (NPs) with fluorophores has been an active area of research for the last two decades with applications in the field of material and biomedical science [12–14]. The fluorescence of a dye

molecule is quenched or enhanced in the close proximity of the metallic nanoparticles by energy transfer or electron transfer. Such fluorescence depend on the size and shape of NPs, and absorption-emission band overlap of the dye molecule with the Plasmon band of the NPs. The emission behavior of a dye molecule can be altered by using metallic nanoparticles and quenching or enhancement of photoluminescence of a dye by silver nanoparticles (AgNPs) depend upon the distance between the dye molecule and NPs [15–17]. The quenching of fluorescence dominates over enhancement at shorter distances and it is attributed to the efficient nonradiative energy transfer between the dye molecule and the metallic NP [18].

The present work describes the photophysical properties of (2*E*)-3-[4-(dimethylamino) phenyl]-1-(naphthalen-1-yl) prop-2-en-1-one (DPNP) in different solvents and fluorescence quenching by silver nanoparticles (Ag NPs) and is a continuation of our systematic studies on the donor-acceptor chalcone derivatives [19–21].

Experimental

Synthesis and Characterization of DPNP

DPNP dye was synthesized by reaction of 4-(dimethylamino) benzaldehyde with 1-acetonaphtone (Scheme. 1). A solution of 4-(dimethylamino) benzaldehyde (1.5 g, 0.010 mol) and 1-acetonaphtone (1.72 g. 0.010 mol) in an ethanolic solution of NaOH (2 g in 20 ml ethanol) was stirred for 3–5 h at room temperature and allowed to stand overnight. The solid product was collected by filtration, dried and recrystallized from ethanol as orange solid (70–78 % yield). The structure of the compound was confirmed by IR, ^{1}HNMR, ^{13}C NMR and X-ray crystallography.

Orange solid, M.pt:195–197 °C; ^{1}H NMR (600 MHz, $CDCl_3$) H: 8.26 (d,1H, J=10.2Hz, ArH), 7.90 (d, 2H, J=10.2 &1.8Hz ArH), 7.95 (d, 1H, J=7.8Hz, ArH), 7.7 (d, 1H, J=3Hz, ArH), 6.7 (d, 1H, J=12Hz, olefinic), 7.09 (d, 1H, J=15.6Hz, olefinic), 7.46 (m,2H,ArH), 7.53-7.50 (m, 4H, ArH), 3.03 (s, 6H, $N(CH_3)_2$); ^{13}C NMR (150 MHz,$CDCl_3$)δ: 196.40,152.14, 147.40,138.15,133.80,130.69,130.48,128.30,127.05,126.41,126.26,125.85,124.80,122.40,122.20,111.80,77.22,76.80; IR (KBr cm^{-1}) ν_{max}=1658, 2910, 1570,1356,1182.

Single crystal of DPNP suitable for X-ray analysis was obtained at room temperature by slow evaporation of $CHCl_3$ solution. One crystal of DPNP (orange 0.17×0.16×0.08 mm) was mounted on Agilent Supernova (Dual source) Agilent Technologies Diffract meter, equipped with a graphite-monochromatic CuKα radiation (λ=1.54184), to collect diffraction data using CrysAlisPro software at 296 K. CCDC (Cambridge Crystallographic Data Centre) reference number 993786 contains the supplementary crystallographic data for this paper and the *ORTEP* diagram of DPNP is shown in Fig. 1. These data can be obtained free of charge at www.ccdc.cam.ac.uk/conts/retrieving.html or from the Cambridge Crystallographic Data Centre, 12 Union Road, Cambridge CB2 1EZ, UK.

Synthesis and Characterization of Silver Nanoparticles

Silver nanoparticles were prepared by the well known chemical reduction method [22]. In a typical procedure, 125 ml of 1×10^{-3} M silver nitrate solution was heated to boiling and 5 ml of 1 % trisodium citrate solution (as nucleating and reducing agent) was added quickly. This resulted in a color change from pale yellow to golden yellow indicating the formation of Ag NPs; stirring was continued until cooled to room temperature. The nanoparticles were characterized by using UV–vis absorption spectrophotometer and Transmission Electron Microscope (TEM). A typical solution of 40–45 nm diameter silver nanoparticles having polygonal shape, exhibiting a characteristic surface Plasmon band around 430 nm was obtained. TEM image of Ag NPs with absorption spectrum shown as an inset is shown in Fig. 2.

Spectral Measurements

All solvents and chemicals used in this work were of spectroscopic grade obtained from Sigma Aldrich and used without further purification. Solvents were checked for the absence of absorbing or fluorescent impurities within the scanned spectral ranges. UV–vis electronic absorption spectra was recorded on a Shimadzu UV-160A spectrophotometer, and the steady-state fluorescence spectra were measured using Shimadzu RF 5300

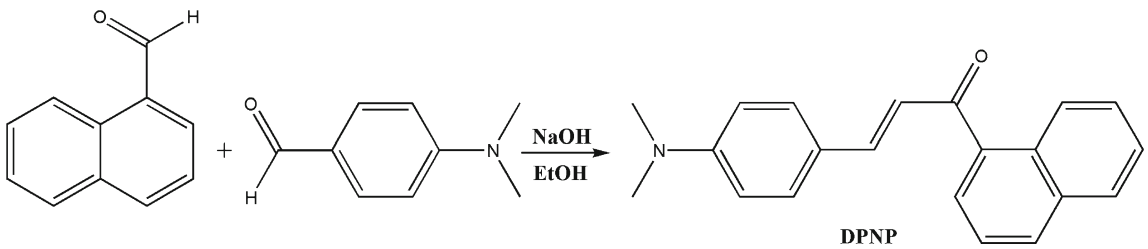

Scheme. 1 Synthetic route of DPNP

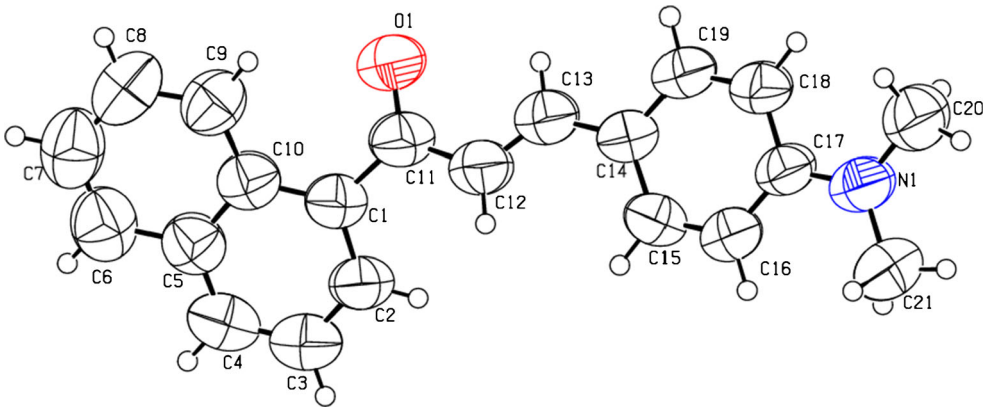

Fig. 1 *ORTEP* diagram of DPNP with thermal ellipsoids drawn at 50 % probability level

spectrofluorphotometer using a rectangular quartz cell of dimensions 0.2×1 cm. The emission was monitored at right angle. The fluorescence quantum yield (ϕ_f) was measured using an optically diluted solution to avoid re-absorption effect (absorbance at excitation wavelength≤ 0.1), relative method with a solution of quinine sulfate in 0.5 mol dm^{-3} H_2SO_4 (φf=0.55) reference standard [23, 24]. The following relation was applied to calculate the fluorescence quantum yield (1):

$$\phi_u = \phi_s \times \frac{I_u}{I_s} \times \frac{A_s}{A_u} \times \frac{n_u^2}{n_s^2} \quad (1)$$

where ϕ_u, ϕ_s are the fluorescence quantum yields of the unknown and standard, respectively, I is the integrated emission intensity; A is the absorbance at excitation wavelength, and n is the refractive index of the solvent.

Results and Discussion

Spectral Behavior of DPNP in Different Solvents

The effect of solvents on the absorption and emission spectra of (1×10^{-5} mol L^{-1}) DPNP in few representative solvents are shown in Figs. 3 and 4, respectively and the corresponding spectral data in detail are summarized in Table 1. The compound show a broad absorption band at 381–412 nm region with a red shift of 31 nm on going from hexane to DMSO indicating that the allowed transition is π-π* with charge transfer character. On excitation at 365 nm, the emission spectrum of DPNP shows a large red shift of 109 nm on changing the solvent polarity from hexane to DMSO. This indicates that photoinduced intramolecular charge transfer (ICT) occurs in the singlet excited state from the electron donating substituent N,N-dimethylamino group to the electron acceptor

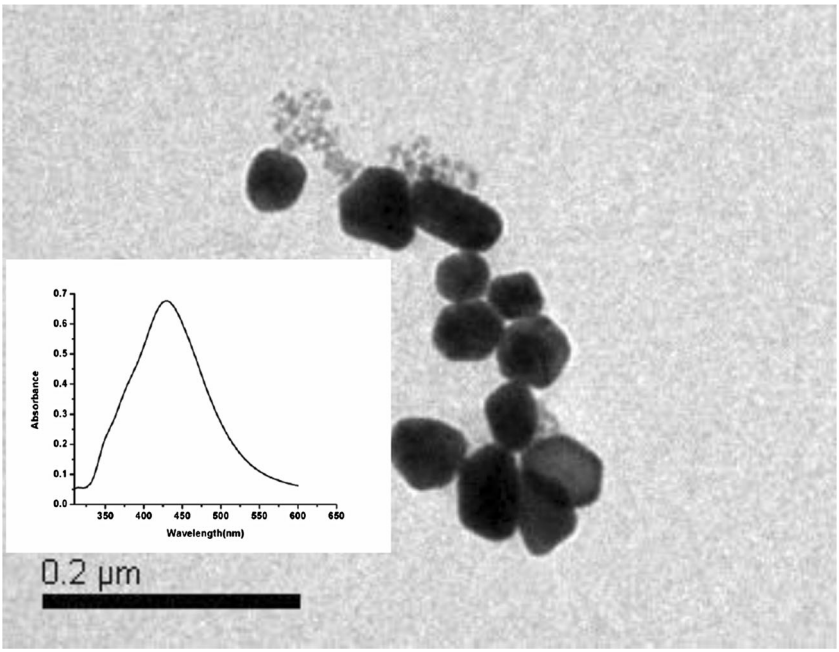

Fig. 2 TEM image of silver nanoparticle. The inset shows the absorption spectrum of Ag NPs

carbonyl group of chromophore and therefore the polarity of DPNP increases on excitation. Further, a considerable difference in the magnitude of Stokes shift was observed from 3975 to 6350 cm^{-1} on changing the solvent polarity from non polar to polar, indicating that the excited state is different from the ground state. As seen in Figs. 3 and 4, absorption spectra show little sensitivity to change in solvent polarity, but emission spectra show a large red shift with increasing solvent polarity, confirming the presence of π-π* transitions in DPNP and stabilization of highly dipolar excited state in polar solvents. The intensity of the emission spectra of DPNP was found to be highest in polar aprotic solvents like chloroform and THF and lowest in polar protic solvents due to solute-solvent interaction such as hydrogen bonding.

The change in dipole moment between the excited singlet state and the ground state ($\Delta\mu=\mu_e-\mu_g$) can be calculated for compounds showing solvatochromic behavior by application of simplified Lippert- Mataga' equation [25, 26]

$$\Delta\overline{\nu}_{st} = \frac{2\left(\mu_e - \mu_g\right)^2}{hca^3}\Delta f + Const. \quad (2)$$

$$\Delta f = \frac{\varepsilon - 1}{2\varepsilon + 1} - \frac{n^2-1}{2n^2+1} \quad (3)$$

where $\Delta\overline{\nu}_{st}$ is the Stokes–shift, which increases with increasing solvent polarity pointing to stronger stabilization of the excited state in polar solvents, h is Planck's constant, c is the speed of light in vacuum, a is the Onsager cavity radius, ε and n are the dielectric constant and refractive index of the solvent, respectively. The Onsager cavity radii (a) from molecular volume of molecules is calculated by using Suppan's Eq. (4) [27].

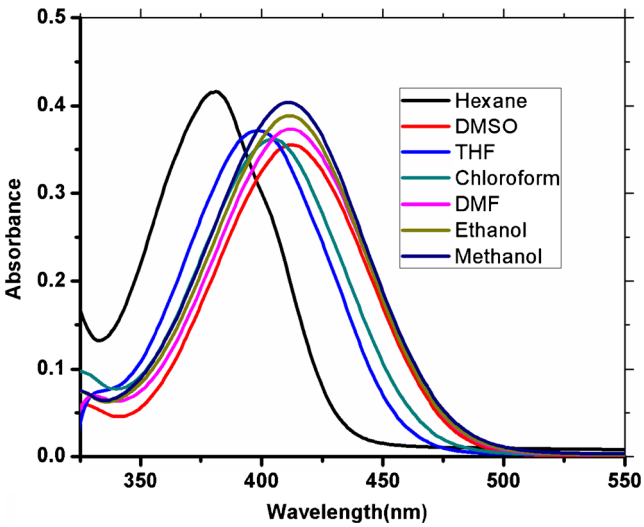

Fig. 3 Electronic absorption spectra of 1×10^{-5} mol L^{-1} of DPNP in different solvents

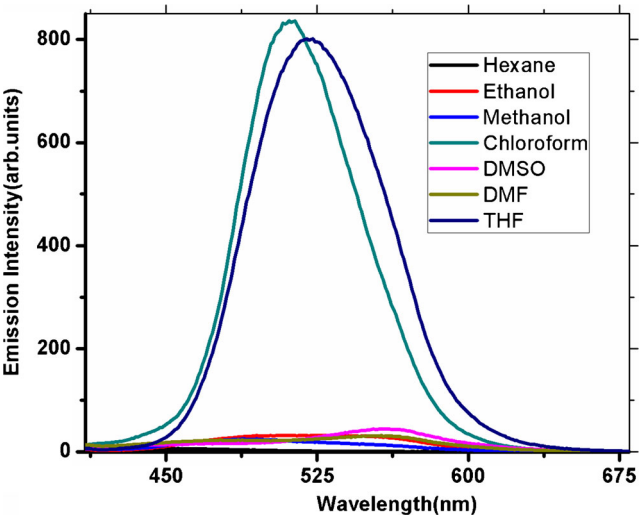

Fig. 4 Emission spectra of 1×10^{-5} mol L^{-1} of DPNP in different solvents (λ_{ex}=365 nm)

$$a = \left(\frac{3M}{4\pi\delta N}\right)^{1/3} \quad (4)$$

where δ is the density (obtained from crystallographic data) of dye, M is the molecular weight of dye and N is Avogadro's number. The value of (a) for DPNP was found to be 4.65 Å. Figure 5 shows the plot of Stokes shift versus the orientation polarization (Δf), and the change in dipole moment of DPNP from the slop of this plot and cavity radius (a) was found to be 7.85 Debye. The data in polar protic solvents were excluded to avoid specific solute-solvent interactions (hydrogen bonding). This change in dipole moment was caused by redistribution of atomic charges in the excited state due to charge transfer from the electron rich-N $(CH3)_2$ groups to the electron acceptor keto-group.

The change in dipole moment ($\Delta\mu$) between the excited singlet and ground state was also calculated using solvatochromic shift method [28, 29] making use of the dimensionless microscopic solvent polarity parameters E_T^N given by the Eqs. (5) and (6),

$$E_T^N = \frac{E_T(solvent)-30.7}{32.4} \quad (5)$$

$$E_T(solvent) = \frac{28591}{\lambda_{max}(nm)} \quad (6)$$

Table 1 Spectral and photophysical parameters of DPNP in different solvents

Solvents	λ_{abs} (nm)	λ_{em} (nm)	$\Delta\bar{\nu}$ (cm^{-1})	ε $M^{-1}cm^{-1}$	Φ_f	f	μ_{12} Debye	$E_T(30)$ K cal mol^{-1}	$\Delta f(D,n)$	E_T^N
Hexane	381	449	3975	41640	0.004	0.778	7.92	31.1	0.0014	0.006
Toluene	395	480	4483	35360	0.1	0.662	7.45	33.9	0.0132	0.099
Heptane	381	450	4024	40040	0.006	0.723	7.64	31.1	0.0004	0.006
DMSO	412	558	6350	35530	0.05	0.664	7.61	45.1	0.263	0.441
Dioxane	396	510	5644	34270	0.34	0.661	7.45	36	0.021	0.164
THF	399	523	5942	37120	0.71	0.714	7.77	37.4	0.210	0.210
Ethyl Acetate	394	518	6075	38000	0.59	0.728	7.80	38.1	0.199	0.230
Acetonitrile	400	550	6818	42600	0.046	0.825	8.36	45.6	0.304	0.472
Chloroform	404	511	5183	36160	0.7	0.667	7.56	39.1	0.148	0.259
DMF	412	554	6221	37340	0.06	0.720	7.93	43.8	0.274	0.404
Butanol	410	541	5905	37320	0.16	0.727	7.95	50.2	0.263	0.506
Propanol	408	544	6127	37180	0.15	0.715	7.86	49.2	0.274	0.570
Ethanol	411	492	4005	38870	0.05	0.754	8.10	51.9	0.288	0.654
Methanol	411	490	3922	40390	0.03	0.783	8.26	55.4	0.308	0.762

where λ_{max} corresponds to the peak wavelength in the red region of the intramolecular charge transfer absorption of the betain dye. In this method, change in dipole moment is calculated from a plot of the Stokes shift versus E_T^N (Fig. 6) according to Eq. (7).

$$\Delta\bar{\nu} = 11307.6\left(\frac{\Delta\mu}{\Delta\mu_D}\right)^2\left(\frac{a_D}{a}\right)^3 E_T^N + Const. \quad (7)$$

$\Delta\mu$ is the difference between the excited and ground state dipole moments of the probe molecule and $\Delta\mu_D$ is the change in the dipole moment of the betaine dye; a (taken as 4.65 Å) and a_D are the Onsager cavity radiia of the probe molecule and betaine molecule respectively. Since the values of a_D and μ_D are known (6.2 Å and 9 Debye, respectively) the change in dipole moment is determined by Eq. (8),

$$\Delta\mu = \left[\frac{81m}{(6.2/a)^3 \times 11307.6}\right]^{1/2} \quad (8)$$

where, m is the slope of linear plot E_T^N *vs* Stokes shift (Fig. 6) which gives $\Delta\mu$=3.48 Debye.

The value of $\Delta\mu$ obtained by Lippert-Mataga's equation is higher than that obtained by dimensionless microscopic solvent polarity parameters E_T^N because it does not consider the polarizability of solute molecules.

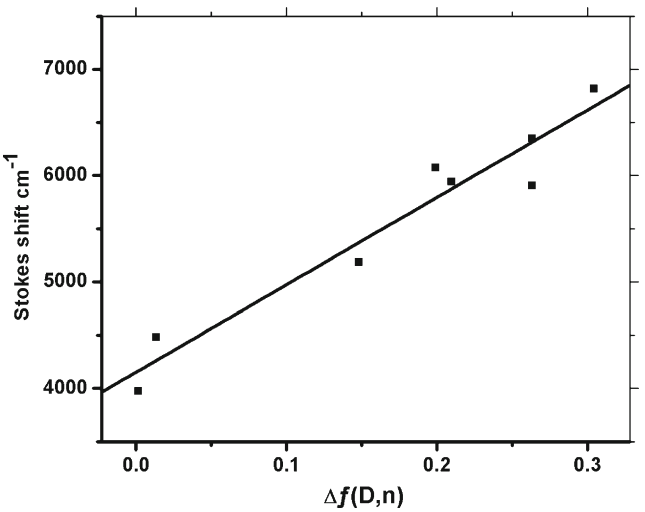

Fig. 5 Plot of ΔF versus Stokes Shift (cm^{-1})

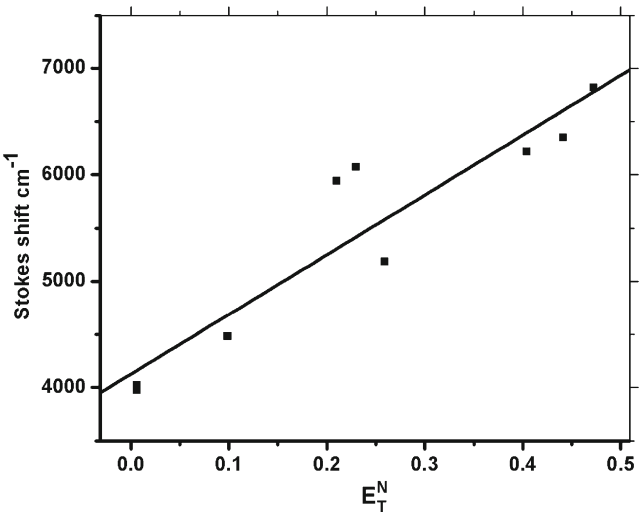

Fig. 6 Plot of E_T^N versus stokes shift (cm^{-1})

The ground to excited state transition dipole moment (μ_{12}) of DPNP in different solvents was calculated using Eq. (9) [30]

$$\mu_{12}{}^2 = \frac{f}{4.72 \times 10^{-7} E_{max}} \quad (9)$$

where, E_{max} is the energy maximum absorption in cm^{-1} and f is the oscillator strength which shows the effective number of electrons whose transition from ground to excited state gives the absorption area of the electronic spectrum. The experimental oscillator strength values were calculated using Eq. (10) [31]

$$f = 4.32 \times 10^{-9} \int \varepsilon\left(\overline{\nu}\right) d\overline{\nu} \quad (10)$$

where, ε is the numerical value for molar decadic extinction coefficient measured in $dm^3\ mol^{-1}\ cm^{-1}$ and $\overline{\nu}$ is the numerical value of the wave number measured in cm^{-1}. The values of f and μ_{12} are listed in Table 1 and indicate that the $S_o \rightarrow S_1$ transition is strongly allowed.

Fluorescence Quantum Yield of DPNP in Different Solvents

The fluorescence quantum yield (ϕ_f) of DPNP is strongly influenced by the polarity and hydrogen bonding ability of the solvents as shown in Table 1. The fluorescence quantum yield can be correlated with the solvent polarity parameter $E_T(30)$ of the solvent, where $E_T(30)$ is the solvent polarity parameter introduced by Reichardt [28], that considers interactions such as solvent polarizability and hydrogen bonding besides those of a specific nature. As depicted in Fig. 7, ϕ_f increases with increase in the polarity of the solvent (expressed as E_T (30)); reaching a maximum in THF with a drop on further increase in the solvent polarity. The large change in the ϕ_f values with the solvent polarity strongly suggests that there is a large structural change for DPNP on photoexcitation in the fluorescent state. The increase in ϕ_f (negative solvatokinetic effect) with charge transfer character was explained by several mechanisms such as proximity effect and conformational changes [32]. The ϕ_f decreases (positive solvatokinetic effect) strongly in highly polar protic solvents because the photo excited dye with ICT state undergo a conversion to a highly polar TICT state by twisting of the molecule around a suitable C-C single bond, making a complete transfer of electrons from donor to acceptor moiety. Stabilization of twisting intramolecular charge transfer (TICT) state from singlet excited state, a concept first introduced by Grabowski [1], is accounted for the reduction of ϕ_f (positive solvatokinetic effect) on going from nonpolar to polar solvents. Moreover, hydrogen bonding between solvent molecules and the carbonyl group of fluorophore plays an important role in the reduction of ϕ_f due to enhanced radiationless processes in highly protic alcoholic solvents [33].

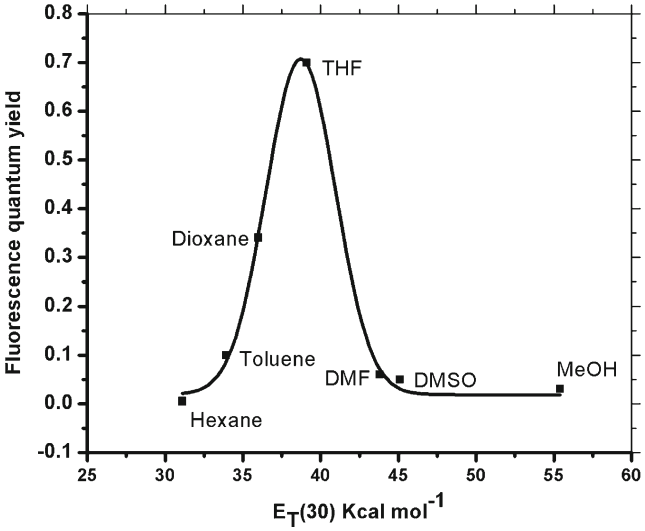

Fig. 7 Plot of $E_T(30)$ versus fluorescence quantum yield

Effect of Acidity in Non-Aqueous Medium on the Electronic Absorption and Emission Spectra of DPNP

The effects of medium acidity on the electronic absorption and emission spectra of DPNP have been studied. The electronic absorption and emission spectra of DPNP (1×10^{-5} mol L^{-1}) in acetonitrile were measured at different pH. In acidic medium a new absorption band develops at 291 nm with an isosbestic point at 348 nm as seen in Fig. 8. The change in absorption spectra of DPNP in acidic media is obviously due to protonation of the N, N-dimethyl amino group. The fluorescence intensity was decreased sharply upon increasing the acidity of medium without any shift in the wavelength of the emission band, due to the formation of the non-emissive protonated form (Fig. 9). The protonation constant of the ground state (pKa) was determined by UV-spectrophotometric titration and fluorimetric titration using the half height method as shown in the inset of Figs. 8 and 9. The values of pKa were determined as 4.3 and 4.6 from absorption and emission spectra, respectively. The excited state protonation constant pKa* was calculated using the following relation (11) [34, 35].

$$pKa - pKa^* = 2.10 \times 10^{-3} \left(\overline{\nu}_{BH^+} - \overline{\nu}_B\right) \quad (11)$$

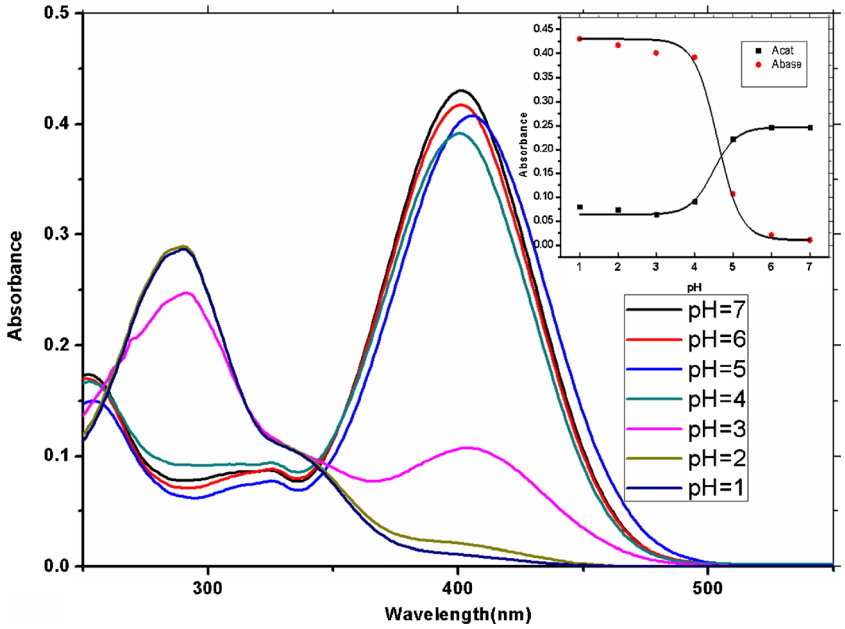

Fig. 8 Electronic absorption spectra of DPNP (1×10^{-5} mol L^{-1}) at different pH. The inset shows the plot of Absorbance versus pH

The quantities ($\overline{\nu}_{BH^+} - \overline{\nu}_B$) represent the difference between the wave numbers of electronic transitions of pure acidic and conjugate base, respectively. The pKa* value observed was 15.21, indicated that the singlet excited state of DPNP is more basic than the ground state.

Fluorescence Quenching Study of DPNP by Silver Nanoparticles

The nature of molecular interaction and microenvironment of fluorophores in solution can be studied by fluorescence quenching experiments. Interaction of silver nanoparticles with DPNP was investigated by fluorescence quenching measurements with variable concentrations of Ag NPs in ethanol and ethylene glycol. The emission spectra of 1×10^{-5} mol L^{-1} solution of DPNP in ethanol and ethylene glycol with different concentrations of Ag NPs are shown in Fig. 10a and b, respectively. On increasing the concentration of Ag NPs, the emission spectrum of DPNP remains unaltered in wavelength but a substantial decrease in fluorescence intensity was observed; which rules out the possibility of ground state complex formation between DPNP and Ag NPs and presence of molecular aggregation.

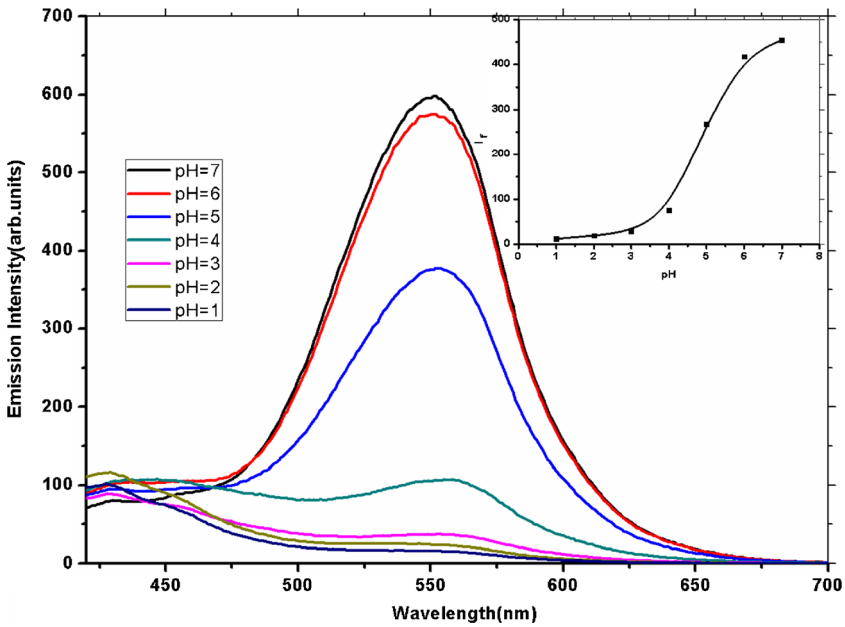

Fig. 9 Emission spectra of DPNP (1×10^{-5} mol L^{-1}) at different pH. The inset shows the plot of Emission intensity versus pH

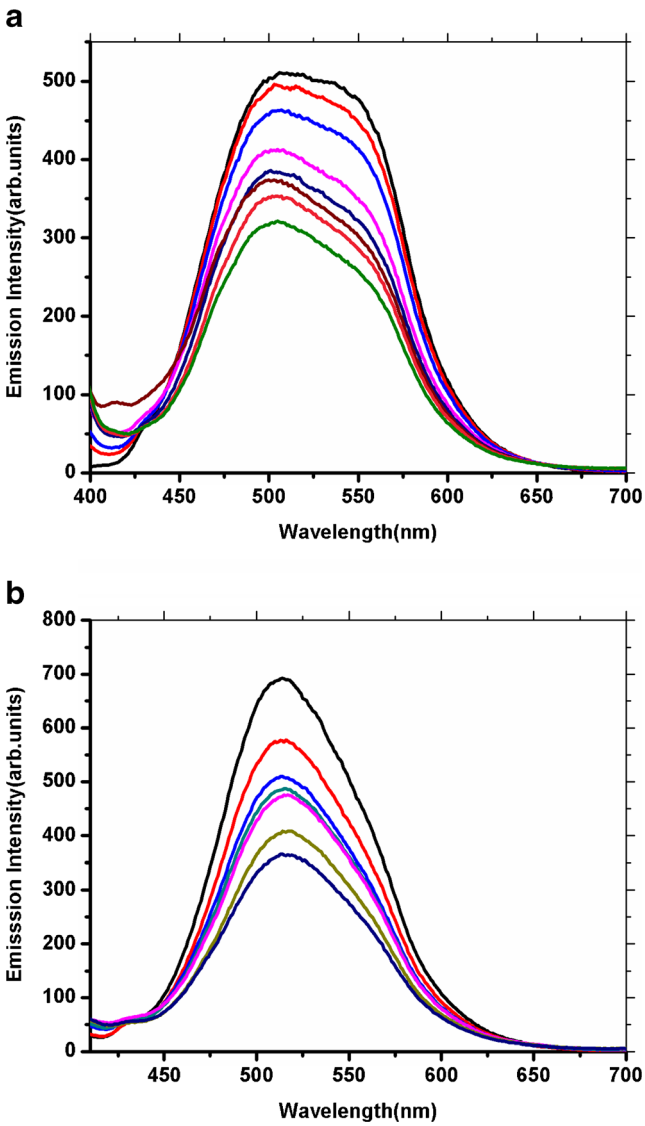

Fig. 10 **a** Emission spectra of 1×10^{-5} mol L^{-1} of DPNP in EtOH in presence of different concentrations of Ag NPs . The concentrations of Ag NPs at decreasing emission intensity are 0.0, 39, 78, 156, 195, 273, 312,and 351 pM (λ_{ex}=380 nm). **b** Emission spectra of 1×10^{-5} mol L^{-1} of DPNP in ehtylene glycol in presence of different concentrations of Ag NPs . The concentrations of Ag NPs at decreasing emission intensity are 0.0, 39, 78, 117, 195, 234, and 312 pM (λ_{ex}=380 nm)

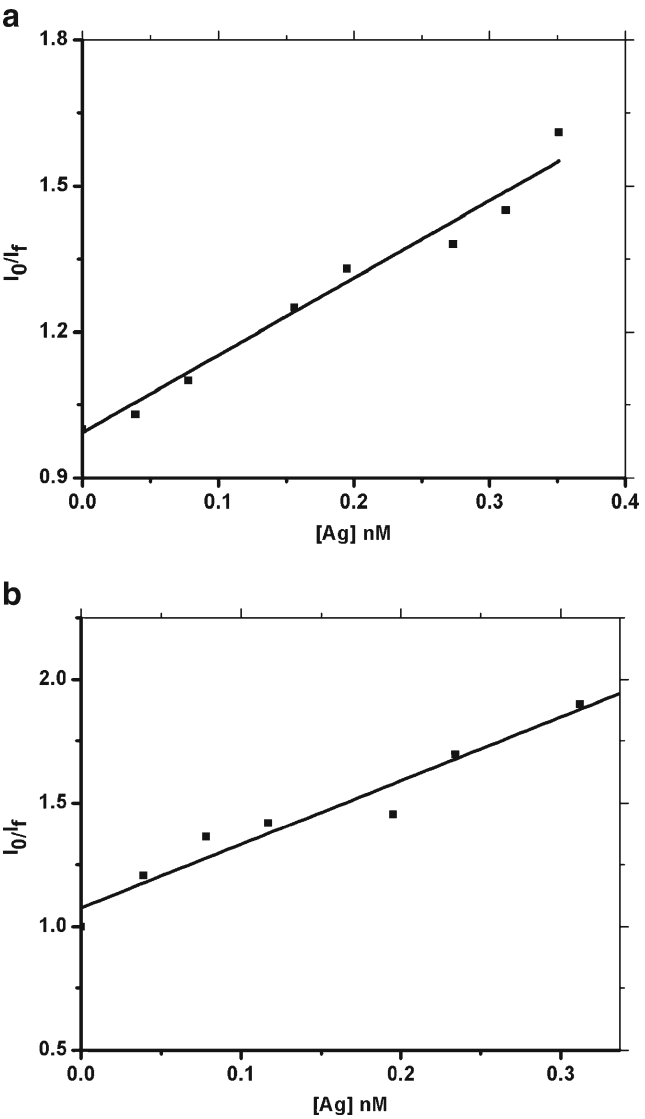

Fig. 11 **a** Stern – Volmer plot for fluorescence quenching of DPNP by Ag NPs in ethanol. **b** Stern – Volmer plot for fluorescence quenching of DPNP by Ag NPs in ethylene glycol

The Stern-Volmer quenching constant (K_{sv}) for DPNP using Ag NPs as quencher were obtained from the Stern-Volmer Eq. (12) [36]:

$$\frac{I_o}{I} = 1 + K_{sv}\ [Ag^o\ ] \qquad (12)$$

where I_o and I are the fluorescence intensities in the absence and presence of the quencher concentration [Ag^o] . he Stern-Volmer plot for DPNP (Fig. 11) was found to be linear with

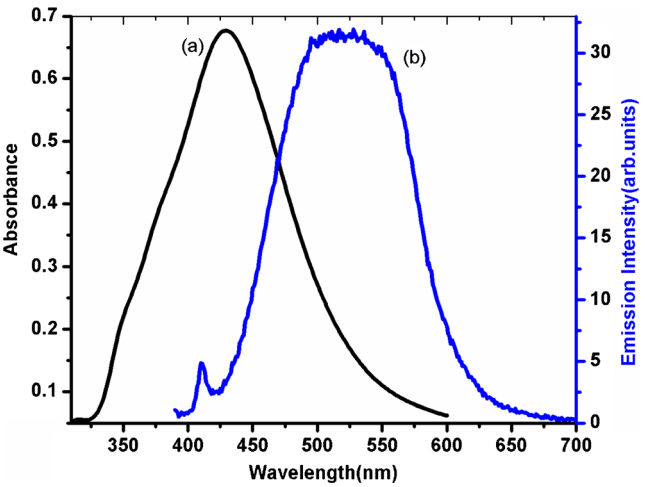

Fig. 12 Spectral overlap of (**a**) absorption spectrum of silver nanoparticles with (**b**) emission spectrum of DPNP

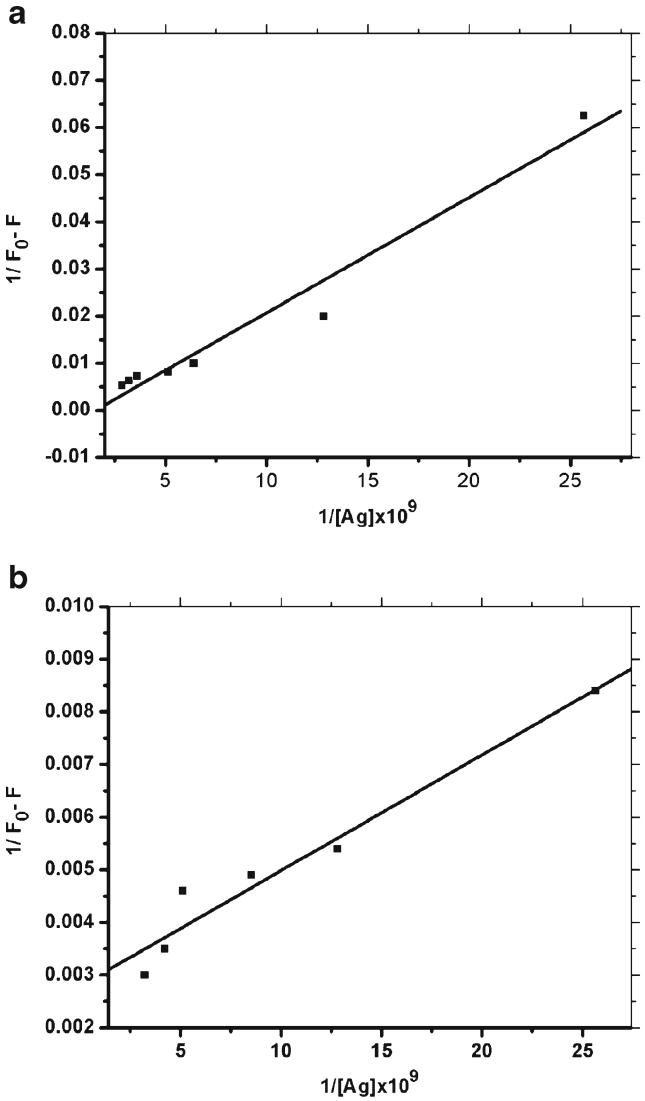

Fig. 13 Benesi – Hildebrand plot for the adsorption of DPNP on Ag NPs: **a** in ethanol and **b** in ethylene glycol

correlation coefficient (R^2) equal to 0.958 and 0.92 in ethanol and ethylene glycol respectively. From the slopes of the linear plots, K_{sv} values were calculated as 1.59×10^9 M^{-1} and 2.57×10^9 M^{-1} in ethanol and ethylene glycol respectively. The higher value for K_{sv} in ethylene glycol implies that quenching efficiency increases as the medium viscosity increases and quenching process is not completely diffusion–controlled. The significant overlap between the emission spectrum of DPNP with the absorption of spectrum of Ag NPs (Fig. 12) reveal the possibility of non-radiative energy transfer from DPNP to Ag NPs according to Forster's theory [37]. Thus, the Stern-Volmer plot and the spectral overlap between the DPNP and Ag NPs indicate the dynamic nature of the quenching process.

The interaction between adsorbed and unadsorbed DPNP molecules was further investigated by determining the apparent association constant (K_{app}) using Benesi–Hildebrand method [38], Eqs. (13–15).

$$\mathrm{DPNP} + \mathrm{Ag} \rightarrow [\mathrm{DPNP} \ldots\mathrm{Ag}] \tag{13}$$

$$k_{app} = [\mathrm{DPNP} \ldots \mathrm{Ag}] / [\mathrm{DPNP}]\,[\mathrm{Ag}] \tag{14}$$

$$\frac{1}{F^o - F} = \frac{1}{(F^o - F')} + \frac{1}{k_{app}} \times \frac{1}{(F^o - F')[Ag]} \tag{15}$$

where, K_{app} is the apparent association constant, F^o is the initial fluorescence intensity of dye molecules, F' is the fluorescence intensity of Ag adsorbed dye and F is the observed fluorescence intensity at its maximum. The calculated values of K_{app} obtained from the plot of $1/F^0$-F vs. 1/ [Ag] (Fig. 13) are found to be 1.72×10^9 and 1.27×10^{10} M^{-1} for ethanol and ethylene glycol, respectively. The higher value of K_{app} indicates the strong association between the DPNP and Ag NPs.

Conclusion

In summary, we have synthesized a new donor-acceptor type chalcone derivative DPNP having intramolecular charge transfer (ICT) characteristics. The structure of this compound was identified by spectroscopy and single crystal X-ray crystallography. A bathochromic shift was observed in the absorption and emission spectrum of DPNP upon increasing the solvent polarity, due to intramolecular charge transfer and intermolecular hydrogen bonding between solute and solvent. Dipole moment calculation results suggest that excited state of DPNP is more polar than the ground state. Physicochemical parameters such as molar absorptivity, oscillator strength, transition dipole moment and fluorescence quantum yield of DPNP have been calculated. The interactions of DPNP with colloidal silver nanoparticles in ethanol and ethylene glycol have also been studied using fluorescence techniques. From the fluorescence quenching data, dynamic quenching and energy transfer from excited DPNP to Ag NPs play a major role in the fluorescence quenching of DPNP by Ag NPs.

Acknowledgments The authors thank the Center of Excellence for Advanced Materials Research and Department of Chemistry at King AbdulAziz University for providing the research facilities. One of the authors, Mehboobali Pannipara is grateful to Deanship of Graduate Studies, King Abdulaziz University for providing PhD Fellowship.

References

1. Grabowski ZR, Rotkiewicz K, Rettig W (2003) Structural changes accompanying intramolecular electron transfer: focus on twisted intramolecular charge-transfer states and structures. Chem Rev 103: 3899–4032
2. Ji S, Yang J, Yang Q, Liu S, Chen M, Zhao J (2009) Tuning the intramolecular charge transfer of alkynylpyrenes: effect on photophysical properties and its application in design of OFF-ON fluorescent thiol probes. J Org Chem 74(13):4855–4865
3. Aoki S, Kagata D, Shiro M, Takeda K, Kimura E (2004) Metal chelation-controlled twisted intramolecular charge transfer and its application to fluorescent sensing of metal ions and anions. J Am Chem Soc 126(41):13377–13390
4. El-Daly SA, Asiri AM, Alamry KA, Obeid AY (2013) UV–visible absorption, fluorescence characteristics and laser activity of (E, E)-2, 5-bis (4-methoxystyryl) pyrazine (BMSP). J Lumin 139:69–78
5. Asiri AM, Khan SA, Al-Amoudi MS, Alamry KA (2012) Synthesis, characterization, absorbance, fluorescence and non linear optical properties of some donor acceptor chromophores. Bull Korean Chem Soc 33(6):1900–1906
6. Acemioğlu B, Arık M, Efeoğlu H, Onganer Y (2001) Solvent effect on the ground and excited state dipole moments of fluorescein. J Mol Struct Theochem 548(1):165–171
7. Cremers DA, Windsor MW (1980) A study of the viscosity-dependent electronic relaxation of some triphenylmethane dyes using picosecond flash photolysis. Chem Phys Lett 71(1):27–32
8. Adeoye MD, Adeogun AI, Adewui S, Odozi NW, Obi-Egbeedi NO (2009) Effect of solvents on the electronic absorption spectra of 9,14 dibenzo (a, c) phenazine and tribenzo (a, c, i) phenazine. Sci Res Essays 4:107–111
9. Inamdar SR, Nadaf YF, Mulimani BG (2004) Ground and excited state dipole moments of exalite 404 and exalite 417 UV laser dyes determined from solvatochromic shifts of absorption and fluorescence spectra. J Mol Struct Theochem 624:47–51
10. Mannekutla JR, Mulimani BG, Inamdar SR (2008) Solvent effect on absorption and fluorescence spectra of coumarin laser dyes: evaluation of ground and excited state dipole moments. Spectrochim Acta A Mol Biomol Spectrosc 69(2):419–426
11. Sidir YG, Sidir I (2013) Solvent effect on the absorption and fluorescence spectra of 7-acetoxy-6-(2,3-dibromopropyl)-4,8-dimethylcoumarin: determination of ground and excited state dipole moments. Spectrochim Acta Mol Biomol Spectros 102:286–296
12. Chhabra R, Sharma J, Wang H, Zou S, Lin S, Yan H, Liu Y (2009) Distance- dependent interactions between gold nanoparticles and fluorescent molecules with DNA as tunable spacers. Nanotechnology 20(48):485201
13. Daniel MC, Astruc D (2004) Gold nanoparticles: assembly, supramolecular chemistry, quantum-size-related properties, and applications toward biology, catalysis, and nanotechnology. Chem Rev 104(1):293–346
14. Deng W, Goldys EM (2012) Plasmonic approach to enhanced fluorescence for applications in biotechnology and the life sciences. Langmuir 28(27):10152–10163
15. Fu Y, Zhang J, Lakowicz JR (2007) Plasmonic enhancement of single-molecule fluorescence near a silver nanoparticle. J Fluoresc 17(6):811–816
16. Kalele S, Deshpande AC, Singh SB, Kulkarni SK (2008) Tuning luminescence intensity of RHO6G dye using silver nanoparticles. Bull Mater Sci 31(3):541–544
17. Rainò G, Stöferle T, Park C, Kim HC, Topuria T, Rice PM, Mahrt RF (2011) Plasmonic nanohybrid with ultrasmall Ag nanoparticles and fluorescent dyes. ACS Nano 5(5):3536–3541
18. Chung HY, Leung PT, Tsai DP (2013) Molecular fluorescence in the vicinity of a charged metallic nanoparticle. Opt Express 21(22): 26483–26492
19. El-Daly SA, Gaber M, El-Sayed YS (2008) Photophysical properties, excitation energy transfer and laser activity of 3-(4'-dimethylaminophenyl)-1-(2-pyridinyl) prop-2-en-1-one (DMAPP). J Photochem Photobiol A Chem 195:89–98
20. Khan SA, Razvi MAN, Bakry AH, Afzal SM, Asiri AM, El-Daly SA Microwave assisted synthesis, spectroscopic studies and non linear optical properties of bis-chromophores. Spectrochimica Acta Part A: Molecular and Biomolecular Spectroscopy. doi:10.1016/j.saa.2014.08.065
21. Pannipara M, Asiri AM, Alamry KA, Salem IA, El-Daly SA (2015) Spectral behavior and photophysical parameters of (2Z)-3-[4-(dimethylamino) phenyl]-2-(4-fluorophenyl) prop-2-ene-nitrile (DPF) in different media. J Lumin 157:163–171
22. Lee PC, Meisel D (1982) Adsorption and surface-enhanced Raman of dyes on silver and gold sols. J Phys Chem 86(17):3391–3395
23. Scaiano JC (1991) Handbook of organic photochemistry. CRC press, Chichester
24. Credi A, Prodi L Inner filter effects and other traps in quantitative spectrofluorimetric measurements: origins and methods of correction. J Mol Structure. doi:10.1016/j.molstruc.2014.03.028
25. Lippert E (1957) Spectroscopic determination of the dipole moment of aromatic compounds in the first excited singlet state. Z Elektrochem 61:962–975
26. Mataga N, Kubota T (1970) Molecular interactions and electronic spectra. Marcel Dekker New York, 371–410
27. Suppan P (1983) Excited-state dipole moments from absorption/fluorescence solvatochromic ratios. Chem Phys Let 94:272–275
28. Reichardt C (1994) Solvatochromic dyes as solvent polarity indicators. Chem Rev 94(8):2319–2358
29. Ravi M, Soujanya T, Samanta A, Radhakrishnan TP (1995) Excited-state dipole moments of some coumarin dyes from a solvatochromic method using the solvent polarity parameter. ENT J Chem Soc Faraday Trans 91(17):2739–2742
30. Coe BJ, Harris JA, Asselberghs I, Clays K, Olbrechts G, Persoons A, Hupp JT, Johnson RC, Coles SJ, Hursthouse MB, Nakatani K (2002) Quadratic nonlinear optical properties of *N*-aryl stilbazolium dyes. Adv Funct Mater 12:110–116
31. Gordon P, Gregory P (1987) Organic chemistry in colour. Chimia, Moskva
32. Rurack K, Dekhtyar MI, Bricks JL, Resch-Genger U, Retting W (1999) Quantum yield switching of fluorescence by selectively bridging single and double bonds in chalcones: involvement of two different types of conical intersections. J Phys Chem A 103: 9626–1935
33. Jana S, Dalapati S, Ghosh S, Guchhait N (2013) Excited state intramolecular charge transfer process in 5-(4-dimethylamino-phenyl)-penta-2,4-dienoic acid ethyl ester and effect of acceptor functional groups. J Photochem Photobiol A Chem 261:31–40
34. Marciniak B, Kozubek H, Paszyc S (1992) Estimation of pKa* in the first excited singlet state. A physical chemistry experiment that explores acid–base properties in the excited state. J Chem Educ 69(3):247
35. Wehry EL (1976) Modern fluorescence spectroscopy. Plenum Press, New York
36. Lakowicz JR (2006) Principles of fluorescence spectroscopy, 3rd edn. Springer, New York
37. Förster T (1996) In: Sinanoglu O (ed) Modern quantum chemistry. Academic, New York
38. Benesi HA HA, Hildebrand JH JH (1949) A spectrophotometric investigation of the interaction of iodine with aromatic hydrocarbons. J Am Chem Soc 71:2703–2707